

DEVELOPMENT OF A NEW HIGH POWER RF WINDOW FOR S-BAND LINAC*

W. H. Hwang[†], Y. D. Joo, B. J. Lee, S. H. Kim, J. Y. Choi,
 Pohang Accelerator Laboratory, Pohang, Korea
 S. J. Roh, Vitzrotech Co., Ltd., Ansan, Korea

Abstract

A prototype rf window was developed in collaboration with Pohang Accelerator Laboratory (PAL) and domestic companies. The PAL designed the S-band TE₀₁₂ rf window and conducted the high power performance tests of single rf window to verify the operation characteristics for the application to the PLS-II Linac. The test was performed in the in-situ facility consisting of a modulator, klystron, waveguide network, vacuum system, cooling system, and rf analyzing equipment. As the test results with SLED, no breakdown appeared up to 75 MW peak power with 4.5 μs rf pulse width at a repetition rate of 10 Hz. The test results with the current operation level of PLS-II Linac confirms that the rf window well satisfies the criteria of PLS Linac operation.

ditioning. After replacing the klystron using a new developed rf window, vacuum recovery time will be reduced from 3 days to 1 day.

We found some rf break-down in existed rf window. There are two parallel rf windows that are in between a 3-dB combiner and a klystron output port. The difficulties of connecting the parts, 3-dB combiner, klystron, and rf windows, causes rf window's distortion. The distortion makes a problem on the surface of ceramic in rf window. The damaged ceramic surface lead to rf breakdowns. In order to eliminate the above problems, we start to develop a new rf windows. In design, the rf window had to be moved to another location to eliminate the parallel connection problem. In order to do that, we need to consider 2 factors that are hardness and rf power capability.

INTRODUCTION

The PLS with 2.5 GeV linear accelerator (Linac) in the Pohang Accelerator Laboratory (PAL) upgraded PLSII machine with 3.0 GeV injector Linac in 2011. Currently, the PLS-II Linac have 17 RF Modules, which is consists of klystron driver, 80 MW klystron, 200 MW Modulator, SLAC energy doubler (SLED), and accelerator structure as shown in Fig. 1 [1], [2].

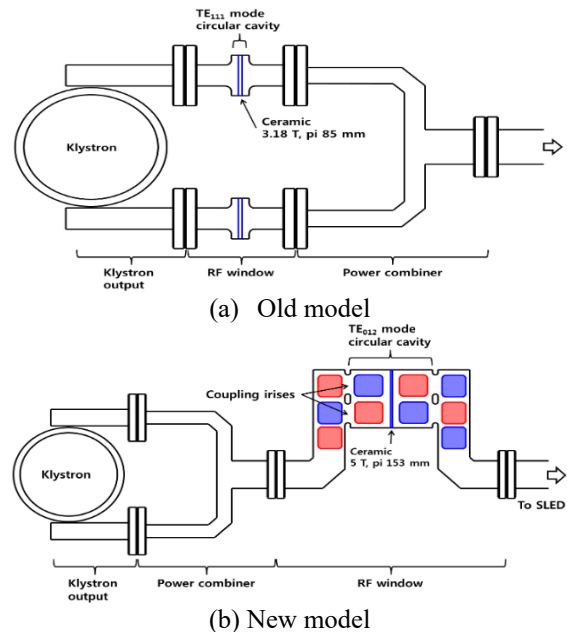


Figure 2: Schematic drawing of klystron module.

Copyright © 2017 CC-BY-3.0 and by the respective authors

Figure 1: Schematic drawing of PLSII Linac rf system.

Two klystron output power goes through the rf windows and then the power is submerged by 3-dB power combiner. And then the combined power is induced to the SLED. The schematic drawing of an accelerator RF module of the PLS-II linac around the klystron output is shown in Fig. 2(a). The TE₁₁₁ pill box cavity rf window separate two vacuum systems between klystron and waveguide. Once a new klystron is replace to an old one, it is hard to increase the power during high power rf con-

DESIGN AND FABRICATION

To reduce the connections of two rf window, the rf window is moved after power combiner as shown in Fig. 2(b). The new location has one connection which reduces the possible improper installation so that a connection problem by distortion of waveguides can be minimized. To protect the ceramic in rf window, the rf window is covered by a solid shell to increase the resistance to physical distortion forces. The power capability of the new rf window has to be twice as much as the former one, which means that the full klystron power goes through the one new rf window. The electric field distribution of a

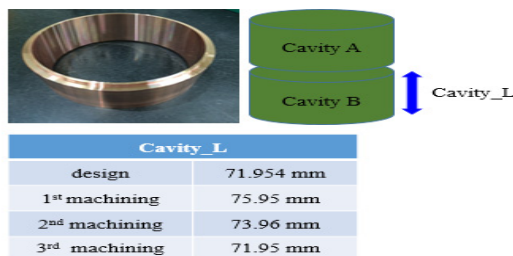
* Work supported by the Ministry of Science, Korea
[†] hohwang@postech.ac.kr

new RF waveguide window is studied by the simulation to estimate the reduction of electric field gradient comparing with that of the former one [3].

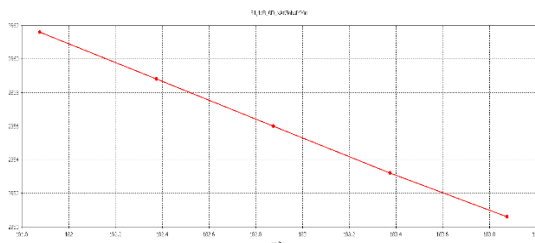
The specification of rf window shows Table 1. The maximum power is 75 MW peak power at a repetition rate of 10 Hz with 4.5 μs rf pulse width. In rf window design, the multipactoring phenomenon on ceramic has to be investigated to reduce the failure of rf window. The ceramic of rf window is damaged by multipactoring mainly. The electric field perpendicular to the alumina ceramic surface (Ez) has more impact on multipactoring than the electric field parallel to the alumina ceramic surface (Et). TE012 mode is selected to reduce the Ez field on ceramic in design [4]. We designed the rf window using CST MWS simulation model [5].

Table 1: Specifications of RF Window

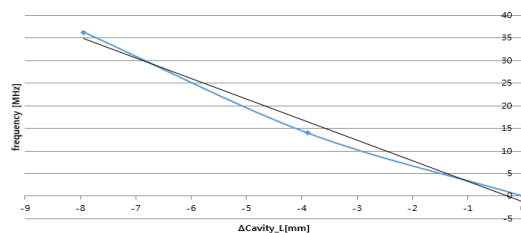
Parameters	Goal
Operating frequency	2856 MHz
Return loss	> 30 dB
Insertion loss	< -0.1 dB
Bandwidth at 25dB	> 10 MHz
RF pulse width	4.5 μs
RF pulse repetition rate	10 pps
RF Peak Power	> 70 MW
Operating temperature	45+/- 0.1 degrees C
Vacuum leak rate	1.0E-10 torr./Sec.



(a) Cavity length



(b) Simulated



(c) Measured

Figure 3: Tuning of cavity length.

The fabrication is processed by VitzroTech Co., in Korea. The resonant frequency of rf window is measured by Network Analyzer. After the fabrication, the resonant frequency was 2820.55 MHz before brazing the rf window. The cavity length is adjusted by machining to find the optimum frequency as shown in Fig. 3(a). Before adjusting the cavity length, the frequency change is simulated according to the cavity length change using MWS code. From the simulation result, the rate of the frequency change by reducing the cavity length is 5 MHz/-1mm as shown in Fig. 3(b). After simulation, cutting out 2mm of the cavity length makes the frequency to change from 2820.55 MHz to 2834.52 MHz. After another 2mm shortening makes the frequency to be 2856.78 MHz. From the above data, the estimation of the frequency rate with regard to the cavity length is 4.5 MHz/-1mm as shown in Fig. 3(c). The schematic drawing of the rf window is shown in Fig. 4. After Brazing, the frequency of the rf window is 2853.21 MHz and 30 dB band width is 6 MHz as shown in Fig 5. The return loss at operating frequency 2856 MHz is 31.4 dB that is over the required designed value, 30 dB. The rf window can be used in the 2856 MHz rf system.

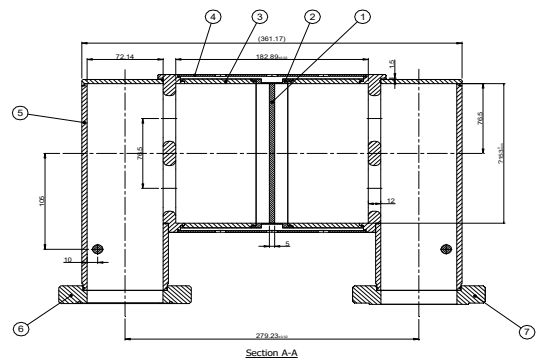


Figure 4: Drawing of rf window.

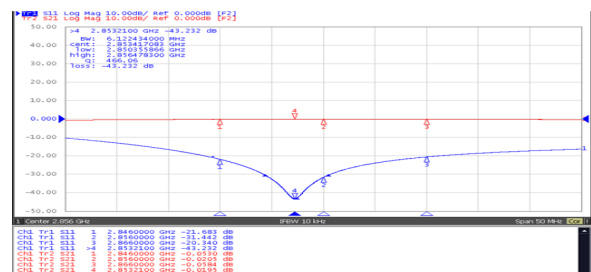


Figure 5: Cold test results of rf window.

HIGH POWER TEST

The high power test for the rf window has been performed with a high power test facility at PAL as shown in Fig. 6. The facility consists of a 2856 MHz signal generator, a 800 W solid state amplifier, a 80 MW Klystron, a 200 MW Modulator, a SLED, a 80 MW Water Load, cold cathode gauges, and beam loss monitors. The vacuum level is monitored using cold cathode gauges (CCG) that are at klystron output port, rf window output, and SLED

output. If vacuum level is increased rapidly at klystron out and rf window output simultaneously, it means that the rf window is source of arcing. Also, arcing by rf breakdown is counted by using Libera beam loss monitor (BLM) and the BLM is installed on the klystron output, the rf window, SLED, and water load [6].

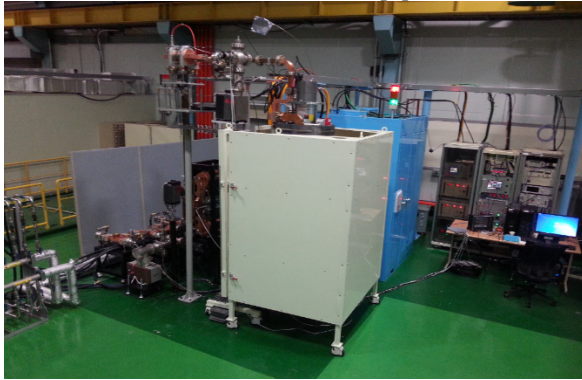


Figure 6: High power test facility.

RF conditioning process starts at the rf power of zero MW with 0.8 μ s rf pulse width and 10 pps rf pulse repetition rate. The klystron output power is controlled by the high voltage (HV) of modulator. When the high voltage reaches to 45 kV, the klystron output power is 75 MW. We increase the HV from 0 kV to 45 kV slowly at 0.8 μ s rf pulse width to prevent the arcing in waveguides and the rf window. Once the HV arrives at 45 kV, the HV is turned off and the rf pulse width is increased slightly. After the increase, the HV processing starts over again. This whole processing keep executed until rf pulse width reaches to 4.5 μ s. The control system studio (CSS) developed by NSLS is used to control the HV and to monitor the vacuum levels. As the power level increases, the vacuum pressure and radiation counts are increased. During the rf processing, no rf breakdown were observed at rf window. Most of the rf breakdowns are occurred at SLED and water load.

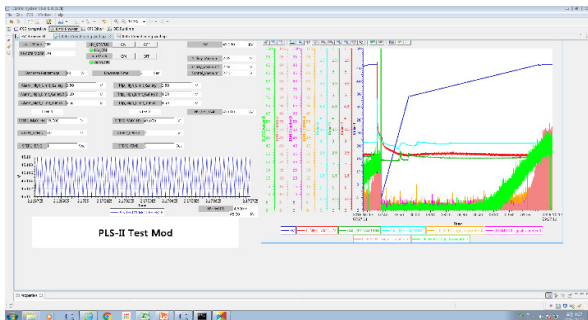


Figure 7: High power test processing with CSS program.

Figure 7 shows rf conditioning process at 4.5 μ s rf pulse width. High voltage of modulator is reached to 45 kV and then the klystron power is 75 MW. Normally, a multi-factoring in copper and ceramic is occurred between 1 MW and 5 MW rf power. The vacuum level of the klystron output port (dark green, named Gallery Vacuum) and rf window output port (sky blue, named Gallery Vacuum 2) is slightly increased at near high voltage of 30 kV that

is equivalent to about 3 MW rf power. It means a multi-factoring has to occur inside of the rf window. But the increased vacuum level is negligible. As an rf power is increased, arcing counts of SLED (red yellow, Counter C) and water load (red yellow, counter D) are increased but no arcing at rf window (pink, Counter B) is observed. Fig. 8 shows waveforms at 45 kV of high voltage with 4.5 μ s rf pulse width. The rf window had a good performance in 75 MW of rf peak power with 4.5 μ s of rf pulse width and 10 pps of rf pulse repetition rate. Furthermore, no rf breakdown and negligible radiation counts were produced in rf window.

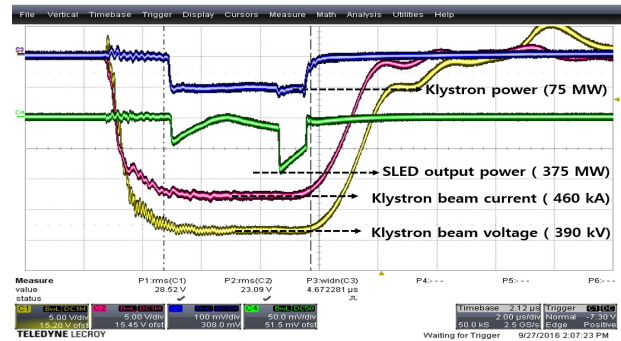


Figure 8: Waveforms of high power test results.

CONCLUSION

The rf window isolate vacuum systems between klystron assembly and waveguide system. Using the new rf window, the recovery time in case of replacing a klystron will be reduced from three days to one day. The design and fabrication of the rf window was successful. The rf window in the high power test succeed as well. Through high power test of prototype of rf window, we confirmed that the rf window had a good performance in 75 MW of rf peak power. To upgrade the operating performance of the PLS-II Linac, the rf window was installed in MK7 module in the early of this year. Until now, the rf window was well functioned.

ACKNOWLEDGEMENT

The authors would like to thank Dr. Matsumoto in KEK for helpful discussions and gratefully acknowledge.

REFERENCES

- [1] S. Shin *et al.*, *J. Instrum.*, vol. 8, p.01019 . 2013.
- [2] B. Lee *et al.*, "PLS-II Linac Upgrade", in Proc of IPAC,12, New Orleans, USA, May 2012, pp.2681-2683.
- [3] A. Miura and H. Matsumoto, "Development of an S-band rf window for linear colliders," *NIM-A*, vol. 334, pp. 341-352, 1993.
- [4] Y. Joo *et al.*, "A new rf window designed for high power operation in an S-band linac rf system.," *J. Korean Phys. Soc.*, vol. 69, No. 6, pp. 1070-1080, 2016.
- [5] CST Microwave Studio User's Manual.
- [6] Beam Loss Monitor User's Manual.